

Cross-kingdom anti-inflammatory effects of fungal melanin on airway epithelium by post-translational blockade of chemokine secretion

Jennifer L. Reedy^{1,2}, Arianne J. Crossen¹, Rebecca A. Ward¹, Christopher M. Reardon¹, Hannah Brown Harding^{1,2}, Kyle J. Basham¹, Jayaraj Rajagopal^{3,4,5,6}, Jatin M. Vyas^{1,2,*}

¹ Department of Medicine, Division of Infectious Diseases, Massachusetts General Hospital, Boston, MA, 02114, USA

² Harvard Medical School, Boston, MA, 02115, USA

³ Center for Regenerative Medicine, Massachusetts General Hospital, Boston, MA, 02114, USA

⁴ Division of Pulmonary and Critical Care Medicine, Department of Medicine, Massachusetts General Hospital, Boston, MA, 02114, USA

⁵ Harvard Stem Cell Institute, Cambridge, MA, 02138, USA

⁶ Klarman Cell Observatory, Broad Institute of Massachusetts Institute of Technology and Harvard, Cambridge, MA, 02142, USA

*Correspondence: jvyas@mgh.harvard.edu

Summary

Respiratory infections caused by the human fungal pathogens, *Aspergillus fumigatus* and *Cryptococcus neoformans*, are a major cause of mortality for immunocompromised patients. Exposure to these pathogens occurs through inhalation, although the role of the respiratory epithelium in disease pathogenesis has not been defined. Employing a primary human airway epithelial model, we demonstrate that fungal melanins potently block the post-translational secretion of CXCL1 and CXCL8 independent of transcription or the requirement of melanin to be phagocytosed, leading to a significant reduction of neutrophils to the apical airway both *in vitro* and *in vivo*. *Aspergillus*-derived melanin, a major constituent of the fungal cell wall, has far-reaching effects, dampening airway epithelial chemokine production in response to fungi, bacteria, and exogenous cytokines. Taken together, our results reveal a critical role for melanin

30 interaction with airway epithelium in shaping the host response to fungal and bacterial
31 pathogens.

32

33 **Keywords:** airway epithelium, *Aspergillus*, melanin, innate immunity, host-pathogen interaction,
34 fungal immunology

35

36

37 Introduction

38 *Aspergillus fumigatus* is the most prominent respiratory fungal pathogen and causes a spectrum
39 of clinical manifestations ranging from allergic disease to severe invasive infections. Despite the
40 ubiquity of this fungal pathogen in the environment, only ~10% of immunocompromised patients
41 (e.g., neutropenic or allogenic bone marrow transplant recipients) develop invasive aspergillosis
42 (IA), indicating that other factors play a significant role in determining the true risk for this
43 infection¹. In addition to infection associated with the immunocompromised state, there is an
44 increased risk of IA following pulmonary viral infections (e.g., influenza, SARS-CoV-2) and in
45 those with underlying lung disease (e.g., asthma, cystic fibrosis [CF], chronic obstructive
46 pulmonary disease [COPD])²⁻⁵. The mortality from *Aspergillus*-related pulmonary disease
47 remains unacceptably high (>50%), coinciding with elevated rates of *Aspergillus* multidrug
48 resistance⁶⁻⁸. Despite this, there is a void in our understanding of the mechanistic interactions
49 governing the invasion of *Aspergillus* at its first point of contact with the host, the airway
50 epithelium.

51 In immune cells, activation of pattern recognition receptors (PRRs), such as the C-type
52 lectin receptor (CLRs), Toll-like receptors (TLRs), NOD-like receptors (NLRs), and Rig-I-like
53 receptors, mediate fungal recognition of cell wall components and subsequent host responses⁹.
54 The cell wall of *Aspergillus* is primarily composed of polysaccharides, including
55 galactosaminogalactan, galactomannan, β -1,3 glucan, β -1,4 glucan, and chitin. Most humans
56 are exposed to *Aspergillus* through the inhalation of conidia, the reproductive propagules of the
57 fungus, which range from 2-3 μ m in size and are easily aerosolized in the environment. In
58 addition to the typical cell wall components, *Aspergillus* conidia are surrounded by a
59 hydrophobic rodlet and 1,8-dihydroxy naphthalene (DHN) melanin layers^{10,11}. Once inhaled by
60 the host, conidia swell and shed these outer layers, exposing the carbohydrate matrix of the cell
61 wall. In immune cells, fungal melanin possesses the remarkable capacity to absorb reactive

62 oxygen species (ROS) and blunt pro-inflammatory cascades, serving as a key virulence factor
63 for many pathogens, including *Aspergillus*¹²⁻¹⁷. Amelanotic strains of clinically relevant fungal
64 pathogens lose their capacity to mount successful infections in mammalian host model systems,
65 indicating that melanin plays a key and non-redundant role in virulence. Indeed, the presence of
66 melanized *Aspergillus* leads to blockage of the phagosome biogenesis¹⁸ and removal of the
67 melanin in the phagosome reprograms macrophage metabolism, promoting an antifungal
68 response¹⁹.

69 Clinical data and current literature indicate that several immune system components are
70 critical for the recognition and swift clearance of fungal pathogens. Still, the rules governing the
71 inflammatory responses to fungi in the lungs are poorly understood. Past studies have focused
72 on innate and adaptive immune cells but have often overlooked a key player in respiratory
73 infections: the airway epithelium - the primary point of contact for inhaled conidia²⁰⁻²³. The
74 conducting airways are sites of *Aspergillus* colonization and invasion²⁰⁻²³. Fortunately, *in vitro*
75 differentiation of primary airway basal cells recapitulates the true diversity of conducting airway
76 epithelium with all of the relevant common (basal, ciliated, club, goblet) and rare (ionocytes, tuft,
77 neuroendocrine) cell types in pseudostratified layers, enabling mechanistic studies in rare
78 populations and the epithelial network in disease²⁴. Additionally, these cells form polarized
79 barriers and enable the investigation of basolateral and apical epithelial responses when grown
80 at air-liquid interface (ALI)^{25,26}. While the primary human airway epithelial cell (hAEC) ALI model
81 may not fully recapitulate the *in vivo* environment (e.g., lacks resident immune cells, endothelial
82 cells, fibroblasts), this model offers the advantages of a highly pliable system to conduct
83 mechanistic studies without compromising relevant human physiology²⁶⁻²⁸ and allow us to
84 pinpoint mechanisms specific to the interaction of the epithelium and inhaled conidia where the
85 microbe first encounters host defense. In addition to utilizing this system, we also use the airway
86 epithelial cell line H292, a mucoepitheliod non-small cell lung carcinoma cell line, which has

87 previously been used extensively in modeling airway epithelial responses to bacterial
88 pathogens. While this cell line does not capture the cellular diversity of the airway epithelium, it
89 is well-suited to mechanistic studies due to cellular uniformity. We previously demonstrated a
90 role for melanin in immune response to *Aspergillus fumigatus* orchestrated by airway epithelium
91 using both primary hAEC and H292 epithelial models²⁶. We observed that airway epithelium
92 infected with *A. fumigatus* lacking DHN melanin promoted greater transepithelial migration of
93 neutrophils than wildtype conidia. The mechanism by which melanin modulates epithelial-
94 mediated neutrophil transmigration remains unknown.

95 In the present study, we leveraged primary hAEC to demonstrate that purified fungal
96 melanin at the apical surface of epithelial cells blocked migration of neutrophils and blunted the
97 apical secretion of chemoattractant chemokines. We determined that DHN melanin suppression
98 of neutrophil transmigration and chemokines occurred in response to both fungal and bacterial
99 pathogens. Furthermore, L-DOPA melanin from *Cryptococcus neoformans* and other
100 commercially available synthetic melanins inhibited CXCL8 (also known as IL-8) secretion,
101 showing these effects were not unique to DHN melanin, but rather is a preserved property of
102 fungal melanins. We determined that fungal melanin abolished the apical-basolateral CXCL8
103 gradient as a mechanism to block neutrophil recruitment. Lastly, we demonstrated that melanin
104 suppressed secretion, but not translation or transcription, of CXCL8 in airway epithelium in a
105 phagocytosis-independent manner. Together, these data indicated that fungal melanin inhibits
106 epithelial-mediated inflammation through blocking the secretion of critical pro-inflammatory
107 chemokines.

108

109 **Results**

110 ***Aspergillus melanin inhibits transepithelial migration of primary neutrophils***

111 We previously demonstrated that hAEC induce neutrophil transmigration upon stimulation with
112 *A. fumigatus* wildtype conidia²⁶. However, induction of neutrophil transmigration required at least
113 4h of infection with *A. fumigatus* in contrast to the bacterial pathogen, *Pseudomonas*
114 *aeruginosa*, which induced robust neutrophil transmigration within 1h²⁶. Furthermore,
115 *Aspergillus* conidia that lacked the ability to produce DHN melanin ($\Delta pksP$) induced neutrophil
116 transmigration within 1h of infection similarly to *P. aeruginosa*, suggesting that melanin was
117 blocking hAEC responses to resting conidia²⁶. Thus, we hypothesized that melanin could act via
118 two mechanisms to block neutrophil migration: melanin could actively downregulate pro-
119 inflammatory responses or serve as a passive barrier to prevent host access to
120 immunostimulatory epitopes on the fungal cell wall. To test these hypotheses, we performed
121 mixing studies with *A. fumigatus* melanin ghosts and amelanotic $\Delta pksP$ conidia. Creation of
122 melanin ghosts is a well-described technique in which melanized conidia are biochemically and
123 enzymatically degraded to strip all cellular components except a rigid shell of purified melanin
124 resembling the original size and shape of the conidia^{18,29-33}. To ascertain whether melanin
125 coating of conidia was required for its inhibitory function, we stimulated primary hAEC with
126 $\Delta pksP$ conidia alone or in combination with melanin ghosts at a ratio of 5:1 melanin ghosts to
127 $\Delta pksP$ conidia then measured neutrophil recruitment across the epithelium. Stimulation of hAEC
128 with $\Delta pksP$ conidia mixed with melanin ghosts dampened neutrophil transmigration when
129 compared to $\Delta pksP$ alone (**Figure 1A**). As expected melanin ghosts alone did not stimulate
130 neutrophil transmigration.

131 We next examined if this response seen in primary hAEC extended to the human lung
132 epithelial cell line, H292, which is routinely used to dissect airway responsiveness to bacterial
133 pathogens³⁴⁻³⁶. While these cells do not recapitulate the cellular diversity of the primary airway
134 epithelium, they are well suited to mechanistic studies given their homogeneity, thus we wished
135 to determine if our phenotype could translate to this model system. We observed that infection

136 with $\Delta pksP$ conidia alone induced more neutrophil recruitment across H292 monolayers
137 compared with $\Delta pksP$ conidia in the presence of melanin ghosts (**Figure 1B**) recapitulating the
138 primary hAECs findings. Since the melanin in these experiments was applied as discrete
139 particles that are unable to coat the surface of the $\Delta pksP$ conidia, these results indicate a model
140 where melanin actively downregulates inflammatory responses rather than acting as a passive
141 barrier on the surface of the conidia.

142

143 ***Aspergillus melanin inhibits airway epithelial-derived CXCL8 and CXCL1***

144 To understand the mechanism of how neutrophil transmigration was silenced, we performed a
145 Luminex assay using primary human airway epithelium derived from three healthy human
146 donors. Primary hAEC was differentiated at ALI for 16 days prior to stimulation with either media
147 alone (HBSS), *P. aeruginosa* (positive control), three wildtype strains of *A. fumigatus* (CEA10,
148 Af293, B5233), or the amelanotic *A. fumigatus* $\Delta pksP$ strain (derived from B5233). CXCL8 and
149 CXCL1 (also known as GRO α) are two neutrophil chemoattractants produced by the airway
150 epithelium and were the most abundant chemokines specifically induced by the mutant $\Delta pksP$
151 *A. fumigatus* strain, but not by wildtype strains (**Figure 2A-B**). We confirmed this difference in
152 cytokine expression in H292 cells using both the $\Delta pksP$ and $\Delta pksP$ complemented strains
153 (**Figure 2C-D**) to validate the use of these cells for mechanistic studies.

154 To determine if melanin acted through a blockade of epithelial chemokine secretion, we
155 performed mixing studies in which we stimulated with a fixed concentration of $\Delta pksP$ conidia
156 combined with graded amounts of melanin ghosts. The mixing assay revealed that the addition
157 of melanin ghosts suppressed both CXCL8 and CXCL1 chemokine production in a dose-
158 dependent manner (**Figures 2E-F**). Melanin ghosts alone applied at the highest concentration
159 did not induce chemokine production.

160

161 ***The inhibitory effects of Aspergillus melanin extend to other pro-inflammatory***
162 ***stimuli***

163 Thus far, our experiments suggested that melanin was not acting as a passive protective shield,
164 but directly downregulated pro-inflammatory responses. We next sought to determine if fungal
165 melanin anti-inflammatory actions were specific to fungal pathogens or if they represented a
166 more general host-microbe interaction. *P. aeruginosa* is an important bacterial respiratory
167 pathogen frequently found in co-infections with *A. fumigatus* in patients with CF. Therefore, we
168 examined whether *Aspergillus* melanin ghosts could dampen *P. aeruginosa*-induced airway
169 epithelial inflammation. We infected H292 monolayers with *P. aeruginosa* alone or in
170 combination with melanin ghosts for 6h then quantified chemokine production. The addition of
171 melanin ghosts suppressed CXCL8 (**Figures 3A**) and CXCL1 (**Figure S1A**) release in response
172 to *P. aeruginosa* in a dose-dependent manner. To ensure that the melanin ghosts were not
173 interfering with the ability of *P. aeruginosa* to bind to the epithelium, we confirmed that *P.*
174 *aeruginosa* binding or internalization by the epithelial cells was not altered in the presence of
175 melanin ghosts (**Figure S1B**), suggesting that the difference in chemokine production was not
176 due to difference in the ability of *P. aeruginosa* to access the cells. Additionally, we performed
177 an LDH cell viability assay that demonstrated no difference in cell viability in the presence of
178 *Pseudomonas* with or without melanin (**Figure S1C**).

179 TNF α is a known inducer of airway epithelial CXCL8, therefore we hypothesized that
180 melanin ghosts also blocks cytokine-induced CXCL8 in airway epithelial cells. We stimulated
181 H292 epithelium with recombinant human TNF α for 6h in the presence of absence of melanin
182 ghosts then quantified CXCL8 production in supernatants. The combination of melanin ghosts
183 and TNF α stimulation of epithelial cells produced less CXCL8 compared to stimulation with
184 TNF α alone (**Figure 3B**).

185

186 ***Melanin blocks Pseudomonas-induced transepithelial migration of neutrophils***

187 Since co-stimulation of airway epithelium with *P. aeruginosa* and melanin ghosts
188 resulted in a potent decrease of CXCL8 secretion, we examined the role of melanin ghosts in
189 airway epithelial-induced neutrophils transmigration in response to *P. aeruginosa*. While CXCL8
190 is a known neutrophil chemoattractant that plays a role in epithelial-induced neutrophil
191 transmigration^{37,38}, recruitment of neutrophils across the epithelium has been linked to other
192 secreted compounds, such as hepoxilin A3, in response to *P. aeruginosa*³⁹⁻⁴². We stimulated
193 both primary hAEC and H292 with *P. aeruginosa* alone or in combination with melanin ghosts
194 and quantified neutrophil transmigration using a myeloperoxidase assay. The addition of
195 melanin ghosts decreased *P. aeruginosa*-induced neutrophil transmigration (**Figure 3C**),
196 demonstrating that melanin blocked all mediators required for neutrophil recruitment to
197 *Pseudomonas*.

198 To determine if the diminished transmigration of neutrophils also occurred *in vivo*, we
199 infected mice with *P. aeruginosa* alone or in combination with melanin ghosts. *P. aeruginosa*
200 induced neutrophil recruitment into the airways of mice, however the number of neutrophils in
201 the bronchoalveolar lavage fluid was decreased in the presence of melanin (**Figure 3D**).
202 Together, these data indicated that modulation of pro-inflammatory processes by melanin
203 ghosts extends to recruitment of neutrophils to the site of infection.

204

205 ***Structurally distinct melanins from diverse sources block airway epithelial CXCL8***
206 ***expression***

207 Melanins are darkly pigmented molecules created through the polymerization of phenol or
208 indole precursors forming polymers of high molecular weight^{43,44}. Despite the ubiquity of melanin
209 pigments across kingdoms (e.g., animals, fungi, insects, helminths), the structure of melanin
210 remains poorly defined. *Aspergillus* and dematiaceous molds produces DHN melanin catalyzed

211 by the polyketide synthase pathway^{13-15,45}. However, some fungal pathogens such as *C.*
212 *neoformans*, an environmental yeast that causes human infections including pneumonia and
213 meningitis, contain melanin derived from L-tyrosine or L-dihydroxyphenylalanine (L-DOPA)
214 produced through the action of tyrosinases^{29,30,46-51}. L-DOPA/tyrosine-based melanins are
215 structurally distinct from *Aspergillus* DHN melanin. This structural differences impact host
216 responses as demonstrated by the recognition of DHN, but not L-DOPA, melanin by the CLR,
217 MelLec or Clec1A, identified on human endothelial and immune cells⁵². To determine if the
218 ability to inhibit the appearance of epithelial-derived CXCL8 in the supernatant was specific to
219 *Aspergillus* DHN melanin, we utilized both *C. neoformans* melanin ghosts and a synthetic
220 tyrosine-based melanin. As strong inducers of epithelial CXCL8, *Pseudomonas* and amelanotic
221 $\Delta pksP$ *A. fumigatus* were used to stimulate H292 epithelium in the presence or absence of *C.*
222 *neoformans* melanin ghosts. Similar to *Aspergillus* melanin ghosts, *Cryptococcus* melanin
223 ghosts suppressed CXCL8 in the supernatant (**Figure 4A**).

224 In addition to our *C. neoformans* melanin ghosts, we also tested epithelial responses to
225 a synthetic source of tyrosine-derived melanin. We previously created fungal-like particles (FLP)
226 using purified fungal carbohydrates which associated with amine-coated polystyrene 3 μ M
227 microspheres using either chemical conjugation or adsorption^{53,54}. Using this technique, we
228 coated beads to create FLP with synthetic L-DOPA and β -1,3 glucan. β -1,3-glucan is a pro-
229 inflammatory carbohydrate found in most fungal cell walls and was added as an additional
230 control to demonstrate that any effect was due to the melanin and not a result of any coating
231 applied to the microspheres. We stimulated H292 monolayers with *P. aeruginosa* either alone or
232 in combination with unmodified FLP (naked beads), L-DOPA melanin-coated FLP, or β -1,3-
233 glucan-coated FLP. We found that combined treatment with *P. aeruginosa* and L-DOPA-coated
234 FLP led to a reduction in CXCL8 secretion, while no difference in CXCL8 secretion was
235 observed when *P. aeruginosa* was combined with either unmodified FLP or β -1,3-glucan-coated

236 FLP (**Figure 4B**). Taken together, these results demonstrate that the immunomodulatory effect
237 of melanin is not specific to *Aspergillus* melanin, but also occurs in response to *C. neoformans*
238 L-DOPA based melanin and a synthetic tyrosine-based melanin.

239

240 **Melanin abolishes the transepithelial gradient of CXCL8 required for neutrophil** 241 **transmigration**

242 Since epithelial cells are polarized, they secrete effector molecules selectively to either the
243 apical or basolateral compartments or bidirectionally. Neutrophil transmigration to the apical
244 surface (*i.e.* airway), requires the creation of a chemokine gradient established by differential
245 secretion at the apical and basolateral surfaces⁵⁵⁻⁵⁷. To understand whether apical stimulation
246 with melanin affected only apical chemokine production or both the apical and basolateral
247 compartments, we stimulated H292 monolayers grown on Transwells with *P. aeruginosa* in the
248 presence or absence of melanin ghosts and collected supernatants from both the apical and
249 basolateral compartments. H292 were chosen to model this interactions because basolateral
250 chemokine production by hAECs, even in the presence of *P. aeruginosa* was at the limit of
251 detection. Stimulation with *P. aeruginosa* induced higher release of CXCL8 on the apical
252 surface of the epithelium when compared to the basolateral surface (**Figure 5A**). The
253 combination of *P. aeruginosa* with *Aspergillus* melanin ghosts significantly decreased both
254 apical and basolateral CXCL8 production when epithelium compared with *Pseudomonas* alone.
255 Furthermore, this co-stimulation effectively abolished the apical-basolateral chemokine gradient
256 generated by *P. aeruginosa*.

257

258 **Melanin induces durable impact on CXCL8 secretion**

259 Thus far, our experiments examined the impact of melanin ghosts for short durations (6h or
260 less). Thus, we sought to understand whether melanin stimulation of epithelium produced a

261 lasting effect at the epithelium or was a transient suppression of chemokine release. Melanin
262 ghosts were durable and were not degraded in our cell culture systems (data not shown). We
263 stimulated H292 epithelium with *P. aeruginosa* or TNF α in combination with melanin ghosts for
264 24h. After 24h stimulation, there was a persistent reduction of CXCL8 production by epithelial
265 cells co-stimulated melanin ghosts compared with either *P. aeruginosa* or TNF α alone (**Figure**
266 **5B**), supporting the hypothesis that melanin silenced the airway epithelium to prevent
267 inflammation, not simply delaying the initiation of response.

268

269 ***Melanin suppression of chemokine production is independent of phagocytosis of***
270 ***melanin or de novo transcription***

271 To determine the mechanism by which melanin blocked CXCL8 production by airway epithelial
272 cells, we first examined whether phagocytosis of melanin ghosts was required. H292 epithelium
273 were pre-treated with cytochalasin D, an inhibitor of actin polymerization that effectively blocks
274 phagocytosis, then stimulated with either TNF α alone or in combination with *Aspergillus* melanin
275 ghosts. Melanin ghosts inhibited TNF α -induced CXCL8 production both in the presence and
276 absence of cytochalasin D, suggesting that phagocytosis of melanin ghosts was not required for
277 its anti-inflammatory action (**Figure 6A**).

278 We next investigated if melanin-induced transcription was required for CXCL8
279 suppression using the transcription inhibitor, actinomycin D. Following pre-treatments with
280 vehicle control or actinomycin D, epithelial cells were incubated with TNF α , TNF α plus
281 *Aspergillus* melanin ghosts, or melanin ghosts alone. TNF α induction of CXCL8 required CXCL8
282 transcription, therefore as expected addition of actinomycin D blocked TNF α induced CXCL8
283 production (**Figure 6B**). Airway epithelial cells produce basal levels of CXCL8 as demonstrated
284 by the media only controls where there was low, but detectable concentrations of CXCL8.
285 Melanin ghosts suppressed basal levels of CXCL8 production by H292 cells. Inhibition of

286 transcription by treatment with actinomycin D, did not alter melanin ghosts-induced suppression
287 of basal CXCL8 (**Figure 6B**). Together, these data revealed that the mechanism via which
288 melanin inhibited CXCL8 production was independent of phagocytosis and *de novo* gene
289 transcription.

290

291 ***Melanin exerts a post-translational blockade on CXCL8 secretion***

292 To understand further how melanin acted at a cellular level, we sought to illuminate the
293 mechanism by which melanin interfered with CXCL8 production by epithelial cells. Therefore,
294 we performed paired experiments, in which we stimulated both primary hAEC cultures (**Figure**
295 **S3A-B**) or H292 monolayers (**Figure 6C-D**) with media alone, wildtype *A. fumigatus* conidia,
296 $\Delta pksP$ conidia alone or in combination with melanin ghosts, *P. aeruginosa* alone or in
297 combination with melanin ghosts, and melanin ghosts alone. CXCL8 transcription was induced
298 by all stimuli compared with media treatment alone and no significant difference in transcript
299 levels between our pro-inflammatory stimuli ($\Delta pksP$ or *P. aeruginosa*) either alone or in
300 combination with melanin, demonstrating that melanin ghosts did not block transcription of
301 CXCL8 (**Figure 6D and S3B**). Immunoblotting of epithelial cell lysates revealed increased
302 intracellular CXCL8 in cells treated with melanin ghosts in combination with a pro-inflammatory
303 stimulant (*i.e.*, $\Delta pksP$ conidia or *P. aeruginosa*) compared to cells treated with the pro-
304 inflammatory stimulant alone (**Figure 6C and S3A**). Interestingly, we observed an increase of
305 intracellular CXCL8 protein within cells treated with melanin ghosts, which is in direct contrast to
306 the decrease in extracellular release of CXCL8 demonstrated by ELISA. These data
307 demonstrated that the difference in extracellular CXCL8 protein in epithelial supernatants was
308 not due to difference in either transcription or translation of the CXCL8 protein. Taken together
309 our results revealed the mechanism of action of melanin on airway epithelial cells. Specifically,
310 melanin interfered with CXCL8 production by airway epithelium through a post-translational
311 blockade of chemokine secretion.

312

313 Discussion

314 Humans are exposed to most fungal pathogens, including *A. fumigatus*, through inhalation of fungal
315 particles including conidia, yeasts, or hyphal fragments. Upon inhalation *Aspergillus* conidia are
316 deposited throughout the host airways, however we lack a fundamental understanding of the role
317 that respiratory epithelium plays in directing the outcome of host-pathogen interaction towards
318 clearance, invasion, or allergic disease. Here, we utilized primary, well differentiated hAEC at ALI
319 and the monomorphic H292 cell line to demonstrate that fungal melanin actively downregulates
320 airway epithelial-driven chemokine responses. Our results demonstrate that *Aspergillus* melanin
321 potently blocks epithelial-driven chemokines via a post-translational inhibition of secretion resulting
322 in the ablation of the chemokine gradient that silences neutrophil transmigration.

323 The primary hAEC model is powerful model as it recapitulates the pseudostratified
324 structure and cellular diversity of conducting airway epithelium, enabling study of rare
325 populations and the interplay of epithelial cells in disease²⁴. Most epithelial cell types cannot be
326 grown in pure cultures, limiting our understanding of the role of specific epithelial cell subtypes
327 in the pathogenesis of disease. While this system has clear advantages over oncogenic and
328 immortalized cell lines, we also confirmed our phenotype in the the cell line, H292, a
329 mucoepitheliod non-small cell lung carcinoma cell line, as this reagent has previously been used
330 extensively in modeling airway epithelial responses to bacterial pathogens^{25,34,35,58-60}. While this
331 cell line does not capture the cellular diversity of the airway epithelium, it is well-suited to
332 mechanistic studies due to uniformity of cellular responses and ability to grow large-scale
333 cultures without a dependence on patient sample quality. Importantly, our results demonstrate
334 that melanin effects both pHAEc and H292 epithelial similarly, indicating that H292 cells can
335 serve as a relevant model system for mechanistic dissection of melanin sensing and response
336 pathways.

337 Prior studies identified an impact on the innate immune sensing of fungal pathogens by
338 fungal melanin. Melanin reprogramed the metabolome of macrophages and prevented LC3-
339 associated phagocytosis of *Aspergillus* conidia through sequestration of calcium preventing
340 calcineurin activation^{19,32,61,62}. Additionally, melanin is a known inhibitor of ROS production by
341 phagocytes¹²⁻¹⁷, which is an important mechanism of pathogen killing by macrophages and
342 neutrophils. Since the airways are the first point of contact in invasive aspergillosis, we sought to
343 determine the biological role melanin played in innate immune responses. Here, we depict a critical
344 role for fungal melanin in decreasing airway epithelial pro-inflammatory chemokine production via a
345 post-translational mechanism, independent of both phagocytosis or *de novo* transcription. The
346 mechanisms responsible for recognition of fungal melanin by epithelial cells and the post-
347 translational pathway contributing to dampened chemokine secretion remains unknown and
348 warrants further studies. MelLec (also known as Clec1A) is a CLR that recognizes *Aspergillus* DHN
349 melanin, but not L-DOPA melanin of *C. neoformans*^{52,61}. Both *A. fumigatus* DHN melanin and *C.*
350 *neoformans* L-DOPA melanin block airway epithelial-derived inflammation suggesting a universal
351 melanin effect at the epithelial surface. Given the specificity of MelLec for only DHN melanin, and the
352 expression of human MelLec is restricted to endothelial cells and innate cells⁵², the respiratory
353 epithelial response to melanin is likely independent of MelLec. Our experiments suggest that the
354 phagocytosis of melanin particles is not necessary, since cytochalasin D does not block the ability
355 of melanin ghosts to suppress epithelial CXCL8 production, suggesting that melanin is interacting
356 with a cell surface receptor or a soluble factor released by epithelial cells. The observations that
357 multiple forms of melanin retain the capacity to blunt the chemokine secretion by airway epithelial
358 cells suggests that human pathogens exploit this pathway to establish successful infection. Indeed,
359 multiple organisms possess melanin including *A. fumigatus*, *C. neoformans*, *Bordetella pertussis*,
360 and *Schistosoma mansoni*⁶³. Our understanding of melanin is evolving from a structural scaffold that
361 provides protection from the harsh environment it inhabits to a multi-purpose molecules that disables
362 the immune response at multiple steps. Our finding that *Aspergillus* melanin inhibits *P. aeruginosa*-
363 induced airway epithelial chemokine secretion indicates that *Aspergillus* could play a role in

364 dampening inflammation during co-infections common in CF patients. Colonization by *Aspergillus*
365 could enhance the virulence of *P. aeruginosa* in patients by blocking early innate immune cell
366 recruitment to sites of *P. aeruginosa* infection.

367 While we focused primarily on CXCL8 for this work, fungal melanin also inhibited the
368 production of CXCL1 (**Figure 2B, S1A, and S2**). While CXCL8 and CXCL1 are known neutrophil
369 chemoattractants that plays a role in epithelial-induced neutrophil transmigration other secreted
370 compounds are also required for *P. aeruginosa* dependent neutrophil transmigration including
371 hepxilin A3³⁹⁻⁴². Melanin ghosts dampened neutrophil transmigration in response to *P.aeruginosa*,
372 indicating that the effect of fungal melanin may have a broad impact on airway epithelial cell
373 secretion. Both CXCL8 and CXCL1 are secreted through the trans-Golgi network. The intracellular
374 accumulation of CXCL8 protein with little detectable extracellular CXCL8 suggests that melanin may
375 interfere with trans-Golgi secretion of CXCL8. Future studies will interrogate both traditional trans-
376 Golgi secretomal pathways, as well as alternative secretion systems, such as IL-1 β which is
377 secreted via a gasdermin dependent mechanism, to determine the extent of the melanin secretional
378 blockade.

379 Fungal melanins act as an anti-inflammatory agent at the respiratory epithelium, blocking
380 post-translational secretion of chemokines to recruit host immune cells. *Aspergillus* melanin is
381 required to establish invasive disease as the $\Delta pksP$ is avirulent in animal models of infection. The
382 mechanism underpinning the virulence defect of the $\Delta pksP$ strain has long been attributed to
383 melanin blockade of phagosomal maturation and ROS production by innate immune cells, critical
384 requirements for host response to *Aspergillus*. However, our work highlights an additional role for
385 melanin in the host-pathogen interaction, as an anti-inflammatory that prevents airway epithelial
386 chemokine secretion thereby decreasing early recruitment of neutrophils to sites of infection. While
387 there is a clear benefit to the pathogen in preventing inflammatory cell recruitment to the airways,
388 there is potential benefit to the host in dampening host response to melanin at the airway epithelium.
389 If melanin fails to silence inflammation in some patients this could lead to chronic inflammatory

390 conditions including chronic pulmonary aspergillosis and allergic diseases such as allergic
391 bronchopulmonary aspergillosis and fungal asthma.

392

393 **Acknowledgements**

394 We would like to thank Drs. Bryan Hurley and Hongmei Mou for insightful discussions regarding
395 our work. Additionally, we would like to thank Dr. George Chamilos for providing melanin ghosts
396 to test in parallel with those created in our own lab. J.L.R is supported by NIH/NIAID grant
397 1K08AI14755. J.M.V is supported by R01AI150181, R01AI136529, and R21AI152499.

398

399 **Author Contributions**

400 *Conceptualization* – Jennifer Reedy and Jatin Vyas. *Investigation* – Jennifer Reedy, Arianne
401 Crossen, Chris Reardon, Hannah Brown Harding. *Writing* – Jennifer Reedy, Rebecca Ward,
402 Arianne Crossen, Jatin Vyas. *Manuscript review and revision* – Arianne Crossen, Hannah
403 Brown Harding, Chris Reardon, Kyle Basham, Rebecca Ward, *Resources* – Jennifer Reedy,
404 Jayaraj Rajagopal and Jatin Vyas.

405

406 **Declaration of Interest:** The authors declare no competing interests.

407

408 **Figure Legends:**

409

410 **Figure 1. *Aspergillus* melanin inhibits transepithelial migration of neutrophils. (A-B)**
411 Neutrophil migration across primary human airway epithelial cells (hAECs) (A) or H292 cells (B)
412 measured by MPO assay following infection (2h hAECs; 1h H292) with $1 \times 10^7/\text{cm}^2$ wildtype
413 B5233 or $\Delta pksP$ *A. fumigatus* conidia in the presence or absence of purified *A. fumigatus*
414 melanin ghosts (MG; $5 \times 10^7/\text{cm}^2$). Negative control of media (HBSS) or MG alone were

415 included. Data represents the number of neutrophils as determined by standard curve. Data are
416 represented as mean \pm SEM. n=4-6; One-Way ANOVA with Tukey's multiple comparisons test;
417 **p<0.01, ***p<0.001, ****p<0.0001.

418

419 **Figure 2. *Aspergillus melanin* inhibits airway epithelial-derived CXCL8 and CXCL1.**
420 CXCL8 and CXCL1 in cell supernatants measured by Luminex (A-B) and ELISA (C-F). (A-B)
421 Primary hAECs following 4h stimulation by media alone (HBSS), *P. aeruginosa* PAO1 strain
422 (PSA), three different wildtype (WT) *A. fumigatus* strains ($1 \times 10^7/\text{cm}^2$) or $\Delta pksP$ *A. fumigatus*
423 conidia ($1 \times 10^7/\text{cm}^2$). n=3. (C-D) H292 cells were stimulated for 4h with HBSS, two WT *A.*
424 *fumigatus* strains, $\Delta pksP$ conidia, or $\Delta pksP$ complemented strain ($1 \times 10^7/\text{cm}^2$). n=4. (E-F) H292
425 were stimulated for 4h with HBSS, WT B5233 conidia ($1 \times 10^7/\text{cm}^2$), $\Delta pksP$ conidia ($1 \times 10^7/\text{cm}^2$),
426 $\Delta pksP$ conidia mixed with increasing concentrations of *Aspergillus melanin* ghosts (MG; 0.1x =
427 $1 \times 10^6/\text{cm}^2$; 1x = $1 \times 10^7/\text{cm}^2$; 10x = $1 \times 10^8/\text{cm}^2$), or MG alone ($1 \times 10^8/\text{cm}^2$). n=3. Data are
428 represented as mean \pm SEM. One-Way ANOVA with Tukey's multiple comparisons test;
429 *p<0.05, **p<0.01, ***p<0.001 compared to $\Delta pksP$ alone.

430

431 **Figure 3. The inhibitory effects of *Aspergillus melanin* extended to other pro-**
432 **inflammatory stimuli.** (A) H292 epithelium infected with media alone (HBSS; negative control),
433 *P. aeruginosa* PAO1 strain (PSA) in the absence and presence of increasing *A. fumigatus*
434 melanin ghosts (MG; 0.2x= $2 \times 10^6/\text{cm}^2$; 1x= $1 \times 10^7/\text{cm}^2$; 5x= $5 \times 10^7/\text{cm}^2$) or MG alone for 6h.
435 CXCL8 secretion in the supernatant was measured by ELISA. n=3. See also Figure S1. (B)
436 CXCL8 secretion was measured by ELISA following a 6h stimulation of H292 cells with HBSS,
437 PSA \pm MG, TNF α (100 ng/mL) \pm MG, or *Aspergillus* MG alone ($5 \times 10^7/\text{cm}^2$). n=3. (C) Neutrophil
438 migration across H292 epithelium in response to PSA alone or in the presence of MG or MG
439 alone ($5 \times 10^7/\text{cm}^2$) was measured by MPO assay. Data represents the number of neutrophils as
440 determined by the standard curve. n=6. (D) 6-12-week-old C57BL/6 mice were infected via

441 oropharyngeal aspiration with PSA (5.85×10^5) with or without *Aspergillus* MG (5.85×10^6) for 4h.
442 The number of neutrophils in the bronchoalveolar lavage fluid was measured by flow cytometry.
443 $n=2-3$. Data are represented as mean \pm SEM. One-Way ANOVA with Tukey's multiple
444 comparisons test; * $p < 0.05$, ** $p < 0.01$, *** $p < 0.001$, **** $p < 0.0001$ compared to stimulation alone
445 (*i.e.*, PSA or TNF α alone).

446

447 **Figure 4. Structurally distinct melanins from diverse sources block airway epithelial**
448 **CXCL8.** (A) H292 cells were stimulated for 6h with wildtype *A. fumigatus* (B5233; $1 \times 10^7/\text{cm}^2$),
449 $\Delta pksP$ conidia ($1 \times 10^7/\text{cm}^2$) with or without *C. neoformans* H99 melanin ghosts (*Cn*-MG)
450 ($5 \times 10^7/\text{cm}^2$), *P. aeruginosa* PAO1 strain (PSA) with or without *Cn*-MG, or *Cn*-MG alone. CXCL8
451 secretion was measured by ELISA. See also Figure S2. (B) H292 epithelium was infected with
452 PSA in the absence or presence of synthetic L-DOPA-coated FLP ($5 \times 10^7/\text{cm}^2$), β -1,3-glucan-
453 coated FLP (BG; $5 \times 10^7/\text{cm}^2$), or naked FLP ($5 \times 10^7/\text{cm}^2$) for 6h, then CXCL8 was measured by
454 ELISA. Media or coated beads alone were included as negative controls. Data are represented
455 as mean \pm SEM. $n=3$; Unpaired t-test; * $p < 0.05$, ** $p < 0.01$, **** $p < 0.0001$ compared to stimulation
456 alone (*i.e.*, $\Delta pksP$ or PSA alone).

457

458 **Figure 5. Melanin abolished the transepithelial gradient of CXCL8 required for neutrophil**
459 **transmigration, with a durable impact on CXCL8 secretion.** (A) CXCL8 expression in the
460 media from the apical (A) and basolateral (BL) sides of H292 cells was measured by ELISA.
461 H292 cells were infected for 6h with *P. aeruginosa* PAO1 strain (PSA) and *Aspergillus* melanin
462 ghosts (MG; $5 \times 10^7/\text{cm}^2$) together or alone. Media alone (HBSS) was used as a negative control.
463 $n=6$; one-way ANOVA with Tukey's multiple comparisons test. (B) An ELISA assessed CXCL8
464 levels following a 24h stimulation with PSA or TNF α (100 ng/mL) in the absence or presence of
465 MG ($5 \times 10^7/\text{cm}^2$). $n=3$; two-way ANOVA with Sidak's multiple comparison test. Data are
466 represented as mean \pm SEM. *** $p < 0.001$, **** $p < 0.0001$.

467
468 **Figure 6. Melanin suppression of chemokine production is independent of phagocytosis**
469 **of melanin or *de novo* transcription, but exerts a post-translational blockade on CXCL8**
470 **secretion.** (A) H292 cells were incubated with DMSO vehicle control or cytochalasin D (CytoD;
471 20 μ M) for 30 min, then stimulated with TNF α (100 ng/mL) and/or *Aspergillus* melanin ghosts
472 (MG; 2x10⁷/cm²) for 6h. Apical CXCL8 levels were measured by ELISA. n=3 (B) H292
473 epithelium was exposed to Actinomycin D (1 μ g/mL), then stimulated as described in A. CXCL8
474 secretion was measured using an ELISA assay. n=3. (C-D) CXCL8 expression in H292 cells
475 lysates was measured by (C) qPCR for RNA and (D) Western blot for intracellular protein,
476 respectively, following 6h stimulation with *A. fumigatus* wildtype (WT; B5233 strain; 1x10⁷/cm²),
477 Δ *pksP* conidia (1x10⁷/cm²) \pm MG, *P. aeruginosa* PAO1 strain (PSA) \pm MG, or MG alone
478 (5x10⁷/cm²). For Western blots, GAPDH was used as a loading control. See also Figure S3.
479 n=2. Data are represented as mean \pm SEM. Unpaired t-test; **p<0.01; ****p<0.0001.

480

481 **Materials and Methods:**

482 **H292 culture, upright and inverted Transwell culture**

483 Human NCI-H292 pulmonary mucoepidermoid carcinoma cell line (H292) (American Type Cell
484 Collection) was grown as previously described^{26,42,58,59}. H292 cells were cultured in complete
485 RPMI medium (cRPMI) (RPMI 1640, L-glutamine, 10% heat-inactivated fetal bovine serum
486 [FBS] (Gibco) and 1% penicillin/streptomycin) at 37°C in the presence of 5% CO₂. For upright
487 Transwell culture, the apical compartments of Costar 6.5 mm or 12mm Transwell® inserts with
488 0.4 μ m pore polyester membrane were treated with a 60% Ethanol, 1:100 rat tail collagen I
489 (Corning) mixture and left open in tissue culture hood for at least 4h to allow for evaporation.
490 H292 cells were then liberated with 0.25% Trypsin-EDTA (Thermo Fisher Scientific) and
491 resuspended in cRPMI. The cell suspension was seeded onto the apical surface of the

492 Transwells and cRPMI was added to the basolateral compartment. For inverted Transwell
493 culture for use in neutrophil migration assays, Costar 6.5 mm Transwell® inserts with 3.0 µm
494 pore polyester membranes (Corning) were inverted and treated with collagen. H292 cells in
495 suspension were applied to the surface of the inverted Transwells to form a small tension
496 bubble and incubated overnight. The following day, Transwells were placed upright in a Costar
497 culture plate (Corning) and both the apical and basolateral compartments were filled with
498 cRPMI. All transwell cultures were incubated at 37°C in the presence of 5% CO₂ and used on
499 day 7.

500 **Primary human airway epithelial basal cell proliferation and upright and inverted ALI** 501 **Transwell Culture**

502 Primary hAEC were grown as previously described^{26,35,64-66}. Basal cells were cultured in small-
503 airway epithelial cell medium (SAGM) (PromoCell) supplemented with 5 µM Y-27632, 1 µM A-
504 83-01, 0.2 µM DMH-1, and 0.5 µM CHIR99021 and 1% penicillin/streptomycin on laminin-
505 enriched 804G-conditioned media coated plates. For differentiation of basal cells into a fully
506 pseudostratified epithelium at ALI, the apical compartments of Costar 6.5 mm or 12mm
507 Transwell® inserts with 0.4 µm pore polyester membrane were coated with 804G-conditioned
508 media for at least 4 hours. Upon removal, a basal cell suspension in SAGM was applied to the
509 apical compartment, and SAGM was added to the basolateral compartment and the transwells
510 were incubated overnight. The following day, the SAGM was replaced with PneumaCult-ALI
511 medium combined 1:1 with Gibco DMEM/F-12 and incubated overnight. The media in the apical
512 compartment was then removed to establish ALI. ALI hAEC were incubated for 16-21 days
513 wherein the apical compartment is kept dry and the ALI media in the basolateral compartment is
514 refreshed frequently.

515 For inverted ALI culture for use in neutrophil migration assays, Costar 6.5 mm
516 Transwell® inserts with 3.0 µm pore polyester membranes (Corning) were inverted and treated

517 with 804G-conditioned media. Basal cells in suspension in SAGM were applied to the surface of
518 the inverted Transwells to form a small tension bubble and incubated overnight. The following
519 day, Transwells were placed upright in a Costar culture plate (Corning) and both the apical and
520 basolateral compartments were filled with SAGM. The following day, SAGM was replaced with
521 PneumaCult-ALI medium combined 1:1 with Gibco DMEM/F-12 and incubated overnight. The
522 media in the apical compartment was then removed to establish air-liquid interface. The inverted
523 ALI were incubated for 16-21 days wherein the apical compartment is kept dry and the media in
524 the basolateral compartment is refreshed frequently. All ALI cultures were incubated at 37°C in
525 the presence of 5% CO₂. Prior to use, the transepithelial electrical resistance (TEER) was
526 measured on the day of experiment to ensure that all epithelium were intact.

527

528 **Fungal and bacterial Culture**

529 *Aspergillus fumigatus* strains Af293, CEA10, B5233, $\Delta pksP$, and $\Delta pksP + pksP$ were used. The
530 B5233, $\Delta pksP$, and complemented $\Delta pksP + pksP$ strains were gifted by K.J. Kwon-Chung
531 (National Institutes of Health; NIH). All *A. fumigatus* strains were grown at 37°C for 3 – 5 days
532 on glucose minimal media slants (GMM). Conidia were harvested by applying a sterile solution
533 of deionized water (Milli-Q, Millipore Sigma, Burlington, MA) containing 0.01% Tween 20 to
534 each slant followed by gentle surface agitation to liberate conidia using a sterile cotton-tipped
535 swab. The solution was passed through a 40 μ m cell strainer to separate conidia from hyphal
536 fragments. Conidia were then washed three times with sterile PBS and counted on a LUNA™
537 automated cell counter (Logos Biosystems). Conidia were used either on the day of harvest or
538 stored at 4°C overnight for use the following day. For animal experiments, conidia were used on
539 the day of harvest.

540 *P. aeruginosa* strain PAO1 was grown overnight in 4 mL of LB liquid media at 37°C with
541 shaking. Cultures were inoculated from frozen stocks of PAO1 stored at -80°C. After shaking

542 overnight, 1 mL of overnight culture was centrifuged at 16,000 g x 5 minutes and washed three
543 times in HBSS. After the final wash the *P. aeruginosa* was resuspended in 600 µl of HBSS. For
544 *in vitro* stimulations, the *P. aeruginosa* was used at a 1:100 dilution. For quantification of
545 bacterial number for *in vivo* experiments, the OD600 of a 1:10 dilution of bacteria in HBSS was
546 obtained and bacteria were diluted appropriately.

547

548 **Neutrophil isolation**

549 Neutrophils were isolated from healthy volunteer donors in accordance with Massachusetts
550 General Hospital IRB-approved protocol (2015P000818) as previously described^{26,59}. Briefly, 50
551 mL of blood was drawn via venipuncture into a syringe containing acid citrate-dextrose. The
552 blood was split between three 50 mL conical tubes and layered on top of a Ficoll-Paque
553 solution, then centrifuged at 2200 rpm for 20 minutes at room temperature to obtain a buffy coat
554 layer. Plasma and mononuclear cells were removed by aspiration. Red blood cells (RBC) were
555 removed using 2% gelatin sedimentation technique followed by a wash with RBC lysis buffer.
556 The remaining neutrophils were washed and resuspended in HBSS without calcium or
557 magnesium (HBSS-) to a concentration of 5×10^7 neutrophils/mL.

558

559 **Neutrophil transmigration experiments**

560 The neutrophil transepithelial migration experiments were performed as previously
561 described^{26,35,36,59}. H292 cell monolayers or primary hAEC were grown on the underside of 3.0
562 µm pore size Transwell filters (Corning Life Sciences) to enable neutrophil migration through the
563 Transwell. Mature epithelium (at least 16 days at ALI for primary hAECs or day 7 monolayers of
564 H292 cells) in 12 well format were used for all experiments. On the day of the experiment,
565 Transwells were equilibrated in HBSS for at least 30 minutes prior to stimulation. Transwells
566 were then inverted into a sterile 15 cm cell culture plate and infected on the apical surface.

567 Cells were stimulated with media only (HBSS), *P. aeruginosa* (PAO1), *A. fumigatus* conidia, or
568 melanin ghosts. Infections were for 1 h on H292 cell monolayers and for 2 h on primary hAEC.
569 After stimulation, the apical surface was washed and transwells were inverted into fresh 24 well
570 culture plates containing HBSS alone or HBSS containing 100 nM *N*-formyl-methionyl-leucyl-
571 phenylalanine (fMLP; Sigma; uninfected positive control). Neutrophils were applied to the
572 basolateral compartment and transmigration was allowed to proceed for 2h (H292 cells) and 4h
573 (primary hAECs) at 37°C with 5% CO₂. After the migration period, the Transwells were
574 discarded and the migrated neutrophils were quantified using a myeloperoxidase (MPO) assay.
575 The migrated neutrophils in the apical compartment were lysed with 0.5% Triton X-100 and
576 neutrophil MPO activity was quantified using a colorimetric assay using citrate buffered 2,2'-
577 azino-bis(3-ethylbenzothiazoline-6-sulfonic acid) diammonium salt (ABTS) solution. After 10 min
578 of incubation, the optical density at 405 nm was read using a spectrophotometer plate reader. In
579 addition, to the experimental samples, a standard curve was prepared for each experiment was
580 used to determine the number of migrated neutrophils based on the OD₄₀₅ value. Data are
581 displayed as the number of transmigrated neutrophils, extrapolated from the standard curve.

582

583 **Melanin ghost preparation**

584 Melanin ghosts were prepared using previously published methods^{18,29-33}. In addition to melanin
585 ghosts created in our lab using the following protocol, we also tested melanin ghosts created in
586 the laboratory of Dr. George Chamilos with similar results to our own. Briefly, *A. fumigatus* strain
587 B5233 was grown for 3□days in T75 flasks (CELLTREAT) on GMM at 30°C. Flasks were
588 seeded from frozen stocks of conidia maintained at -80°C. To harvest conidia, a sterile solution
589 of deionized water (Milli-Q; Millipore Sigma) containing 0.01% Tween 20 (Sigma-Aldrich) was
590 added to each flask, and spores were liberated using gentle surface agitation with a sterile
591 swab. The spore solution was passed through a 40-μm cell strainer to separate hyphal debris.

592 To remove the fungal cell wall, spores were washed three times with sterile PBS, then
593 resuspended in 10mg/mL lysing enzymes from *Trichoderma harzianum* which has since been
594 discontinued and replaced with 5mg/mL lyticase from *Arthrobacter luteus* (Sigma-Aldrich)
595 dissolved in a 1 M Sorbitol (Sigma-Aldrich) / 0.1 M Sodium Citrate (Sigma-Aldrich) solution in
596 deionized water. The solution was incubated in a 30°C water bath for 24h. To denature proteins,
597 the spore solution was then washed twice with sterile PBS and resuspended in a 4 M guanidine
598 thiocyanate (Sigma-Aldrich) solution and incubated at room temperature for 18h with nutation.
599 To hydrolyze proteins, spores were then washed twice with sterile PBS and resuspended in a
600 1.0 mg/mL Proteinase K (Roche Laboratories) in 10mM Tris-HCl (Sigma-Aldrich), 1mM CaCl₂
601 (Sigma-Aldrich), and 0.5% Sodium Dodecyl Sulfate (Sigma-Aldrich) pH 7.8, solution in distilled
602 water. The suspension was incubated in a 65°C water bath for 4h, then washed three times with
603 sterile PBS and resuspended in a 0.9% NaCl solution. A Folch lipid extraction was then
604 performed wherein the suspension was transferred to a separatory funnel along with methanol
605 (Thermo Fisher Scientific) and chloroform (Midland Scientific) and mixed vigorously. This was
606 repeated twice, with the organic layer being drained each time and the soluble melanin-
607 containing interfacial layer maintained. For the hydrolysis of residual acid-labile constituents, 6M
608 HCl (Thermo Fisher Scientific) was added to the flask and boiled for 1 hour, then combined with
609 equal volume sterile PBS to neutralize pH. The melanin ghost suspension was then washed
610 with sterile PBS and placed in 0.22 µm centrifugal filter units (Merck Millipore Ltd). The melanin
611 ghosts were then washed 3 times and resuspended in deionized water. The suspension was
612 frozen overnight at -80°C and lyophilized for two days. The melanin ghosts were finally
613 resuspended in sterile PBS, sonicated, and counted on a LUNA automated cell counter (Logos
614 Biosystems).

615

616 **Fungal-like particle (FLP) creation**

617 We have previously created FLP using purified fungal carbohydrates which we can associated

618 with amine-coated polystyrene 3 μ M microspheres using either chemical conjugation or
619 adsorption^{53,54}. To create melanin-coated particles, synthetic melanin (Sigma) was sonicated
620 robustly in DMSO to create a fine suspension that was then incubated with amine-coated
621 polystyrene microspheres for 1h at room temperature with shaking. The microspheres were
622 washed copiously with PBS to remove all traces of DMSO and free melanin particles. All of the
623 microspheres obtained a brown coloration consistent with melanin association and there was no
624 free melanin visible in the flow through from the FLP.

625

626 **ELISA**

627 Mature epithelium (at least 16 days at ALI for primary hAECs or day 7 monolayers of H292
628 cells) in either 12 or 24 well format were used for all experiments. On the day of the experiment,
629 growth media was removed and cells were equilibrated for at least 30 min in HBSS. HBSS was
630 removed and replaced with fresh HBSS alone or containing the appropriate stimulants. Since
631 the primary hAEC are pseudostratified epithelium, the concentration of applied stimuli was
632 based upon the surface area of the epithelium rather than an MOI calculation. After application
633 of stimuli, cell culture plates were spun gently at 1000 rpm x 5 min to bring pathogens in contact
634 with epithelial surface. Stimulations were allowed to proceed for the desired time (4h – 24h).
635 Supernatants were harvest and centrifuged through Captiva 96 well 0.2 μ M filter plate at 3000
636 rpm for 10 min. Supernatants were frozen at -80°C until use. ELISAs were performed using
637 either R&D Duoset kits or Biolegend LegendPlex assays according to the manufacturers
638 instructions. For the R&D Duoset kits the ELISA were read using an i3X Spectrophotometer
639 (Molecular Devices, LLC). For the LegendPlex assays, a BD FACSCelesta™ Flow Cytometer
640 (BD) was used for data acquisition. The resultant flow cytometry files were then analyzed using
641 the LEGENDplex™ Data Analysis Software Suite. Results were analyzed using GraphPad

642 PRISM9 software (GraphPad Software). All reported ELISAs were done in both technical and
643 biological triplicate.

644 For cytochalasin D experiments, cytochalasin D was added to HBSS media at a final
645 concentration of 20 μM . Epithelial cells were incubated for 30 min at 37°C prior to stimulation. At
646 that time the media was exchanged for fresh HBSS containing the indicated stimulants in
647 addition to 20 μM cytochalasin D. To inhibit transcription, actinomycin D dissolved in DMSO was
648 added to HBSS at a final concentration of 1 $\mu\text{g}/\text{mL}$. An equal volume of DMSO in HBSS was
649 added to the control wells. Epithelial cells were then incubated for 1h at 37°C prior to
650 stimulation.

651

652 ***In vivo* neutrophil recruitment experiment**

653 C57BL/6 mice of 6 -12 weeks of age were obtained from Jackson Laboratories and housed in
654 the Massachusetts General Hospital specific pathogen-free animal facilities for at least one
655 week prior to infection. *Pseudomonas* strain PAO1 was diluted and quantified using OD600.
656 Inoculums were prepared consisting of HBSS alone, 5.8×10^5 CFU PaO1 alone, 5.9×10^6
657 melanin ghosts alone, or a 5.8×10^5 CFU PAO1 combined with 5.8×10^6 melanin ghosts. Each
658 inoculum was prepared in 50 μl total volume in HBSS. Mice were infected via oropharyngeal
659 aspiration of the inoculum under isoflurane anesthesia. Infection was allowed to proceed for 4
660 hours, at which time mice were euthanized using CO_2 . Mice were exsanguinated, and the
661 trachea was exposed and cannulated with a 22G catheter (Exel Safelet Catheter) that was
662 secured in place using suture string. The lungs were flushed with a total of 2.3 ml of PBS
663 containing 5% fetal bovine serum. The collected bronchoalveolar lavage fluid was centrifuged at
664 300 g x 5 min to pellet cells. The pelleted cells were resuspended in FACS buffer (PBS + 2%
665 bovine serum albumin) containing 1:100 dilution of Fc Block and a 1:250 dilution of Zombie
666 Violet dye. After incubation at 4°C for 15 minutes, cells were centrifuged and then resuspended

667 in FACS buffer containing an antibody cocktail consistent of anti-CD11b APCFire, anti-CD45
668 BV605, and anti- Ly6G AF488. After incubation at 4°C for 20 min cells were washed with FACS
669 buffer and then fixed in 4% paraformaldehyde for 10 min at room temperature. Cells were
670 washed and then resuspended in FACs buffer and stored at 4°C (cells were stored no longer
671 than overnight prior to flow cytometry). Splenocytes for a single mouse were prepared in parallel
672 to use as controls for flow cytometry gating. Counting beads were added prior to flow and
673 calibration beads were prepared using each of the fluorophores. Samples were run on a a BD
674 FACSCelesta™ Flow Cytometer, and analysis was performed using FlowJo 10 software (BD).
675 Three mice were used per experimental group. All animal studies were conducted under
676 protocols approved by the Institutional Animal Care and Use Committee Subcommittee on
677 Research Animal Care at Massachusetts General Hospital.

678

679 **RNA extraction and qRT-PCR**

680 Epithelium was grown on 0.4 µm pore-size Transwells until mature (at least 16 days hAEC or 7
681 days for H292 cells). On the day of stimulation, media was removed and cells were equilibrated
682 in HBSS for at least 30 min prior to stimulation with either media alone (HBSS), *Pseudomonas*
683 *aeruginosa* (PAO1), *A. fumigatus* conidia or melanin ghosts alone or in combination. Conidia
684 were applied at 1×10^7 conidia per cm^2 and melanin ghosts were applied at 5X concentration at
685 5×10^7 conidia per cm^2 . After 6h of stimulation, supernatants were harvested for ELISA. At least
686 4 Transwells of epithelium were stimulated per condition, one well of epithelium was used for
687 Western blot analysis and three wells were each harvested for RNA. For RNA prep, the
688 epithelium was washed with ice-cold HBSS and then RNA was isolated using the QIAGEN
689 RNeasy Mini Kit. After harvest of cell lysates in QIAGEN RLT buffer containing beta-
690 mercaptoethanol, cell lysates were transferred to QIAGEN QIAshredder columns to homogenize
691 the cells, the rest of the RNA extraction was performed according to RNeasy mini kit

692 instructions. RNA was quantified using nanodrop. cDNA was created using the SuperScript IV
693 VILO kit (Thermo Fisher Scientific) according to manufacturers instructions. qRT-PCR was
694 performed on cDNA using the Taqman[®] Fast Advanced Master Mix and Taqman[®] Gene
695 Expression assay probes CXCL8 labelled with FAM and GAPDH labelled with VIC-MGB. qRT-
696 PCR reactions were run using the Applied Biosystems™ 7500 Fast Real-Time PCR System per
697 kit instructions and analyzed using the $\Delta\Delta C_t$ method. All qRT-PCR experiments were performed
698 in at least biological duplicates.

699 **Western blot**

700 Epithelium were prepared as described in “RNA extraction and qRT-PCR”. After 6h of
701 stimulation the epithelium was placed on ice and lysed with 1% NP40 lysis buffer containing
702 protease inhibitor. Following denaturation with NuPAGE LDS Sample Buffer (Thermo Fisher
703 Scientific) proteins were resolved by SDS-PAGE on NuPAGE gels (NuPAGE gels, Thermo
704 Fisher Scientific). Proteins were then transferred to methanol-activated PDVF membrane
705 (Perkin Elmer) using transfer buffer (0.025M Tris, 0.192 M glycine, 20% methanol) and
706 electrophoretic transfer at 100V for 1h. The membranes were blocked for 1h at room
707 temperature in 5% Milk in PBS-0.01% Tween 20 (PBST), and then incubated with anti-CXCL8
708 antibody overnight at 4°C. Membranes were washed and incubated for 1h at room temperature
709 with secondary HRP conjugated antibody. After washing, membranes were visualized using
710 Western Lightning Plus ECL chemiluminescent substrate (Perkin Elmer, Waltham, MA) and
711 developed using Kodak BioMax XAR film (Millipore Sigma). Films were then scanned and
712 processed using Adobe Photoshop 2021. Any contrast adjustments were applied evenly to the
713 entire image and adheres to the standards set forth by the scientific community⁶⁷. All reported
714 western blots were repeated in at least biological duplicate.

715 **Luminex assay**

716 24- well Transwells were prepared using basal epithelial cells from three healthy human donors
717 and differentiated for 16 days at ALI. On the day of stimulation, ALI media was removed and
718 epithelium were equilibrated in HBSS media for 1.5h prior to stimulation. The HBSS was
719 removed and replaced with fresh HBSS media on the basolateral side, and 200 μ L of HBSS
720 media containing $1 \times 10^7/\text{cm}^2$ wild type conidia (strains CEA10, Af293, B5233), $\Delta pksP$ conidia or
721 *P. aeruginosa* strain PAO1. After 4h, the apical and basolateral media was harvested and put
722 through a Captiva 96 well 0.2 μ m filter plate at 3000 rpm for 10 min. Supernatants were frozen
723 at -80°C . Data were processed using the Luminex analytical software. MILLIPLEX Map Human
724 cytokine/chemokine Magnetic Bead Panel – Premixed 41 Plex, run on a MAGPIX[®] xMAP
725 instrument according to manufacturer’s instructions. Analysis was performed using GraphPad
726 Prism.

727 **Pseudomonas epithelial association assay**

728 H292 epithelium were infected with PAO1 alone or in combination with 5×10^7 *Aspergillus*
729 melanin ghosts and incubated for 4h. Wells were washed three times with HBSS to remove any
730 nonadherent bacteria. To lyse epithelial cells, 1% Triton X-100 was added to each well, and
731 plates were incubated with gentle agitation for 1h at 4°C . The lysate was collected, vortexed,
732 and 1:10 serial dilutions were made in HBSS. 100 μ L of each dilution was plated onto LB agar
733 plates containing ampicillin and spread using glass beads. The plates were incubated at 37°C
734 overnight and colony forming units were counted the following day.

735

736 **LDH viability assay**

737 The LDH viability assay was performed using Invitrogen CyQUANT LDH Cytotoxicity Assay
738 according to the manufacturers instructions. After 6h infection of H292 cells, a 1:10 dilution of
739 1% Triton X-100 was added to control well containing unstimulated epithelium to lyse the cells

740 and incubated for 10 min at 37°C 5% CO₂. 50 µL of supernatant from each experimental
741 condition (all experimental conditions were performed in triplicate) was transferred to a 96 well
742 plate and mixed with 50 µL of the kit Reaction mixture and allowed to incubated for 30 min at
743 room temperature in the dark. Stop solution was then added to each sample and absorbance at
744 490 and 680 was measured using an i3X Spectrophotometer (Molecular Devices, LLC). LDH
745 activity and % cytotoxicity were calculated according to assay kit instructions.

746

747

748

749

REFERENCES

750

751 1. Thompson, G.R., 3rd, and Young, J.H. (2021). *Aspergillus* infections. *N Engl J Med* *385*,
752 1496-1509. 10.1056/NEJMra2027424.

753 2. Huang, L., Zhang, N., Huang, X., Xiong, S., Feng, Y., Zhang, Y., Li, M., and Zhan, Q.
754 (2019). Invasive pulmonary aspergillosis in patients with influenza infection: A
755 retrospective study and review of the literature. *Clin Respir J* *13*, 202-211.
756 10.1111/crj.12995.

757 3. Rawson, T.M., Moore, L.S.P., Zhu, N., Ranganathan, N., Skolimowska, K., Gilchrist, M.,
758 Satta, G., Cooke, G., and Holmes, A. (2020). Bacterial and fungal coinfection in
759 individuals with coronavirus: a rapid review to support COVID-19 antimicrobial
760 prescribing. *Clin Infect Dis* *71*, 2459-2468. 10.1093/cid/ciaa530.

761 4. Rayens, E., Norris, K.A., and Cordero, J.F. (2021). Mortality trends in risk conditions and
762 invasive mycotic disease in the United States, 1999-2018. *Clin Infect Dis* *74*, 309-318.
763 10.1093/cid/ciab336.

764 5. Takazono, T., and Sheppard, D.C. (2017). *Aspergillus* in chronic lung disease: modeling
765 what goes on in the airways. *Med Mycol* *55*, 39-47. 10.1093/mmy/myw117.

766 6. Bueid, A., Howard, S.J., Moore, C.B., Richardson, M.D., Harrison, E., Bowyer, P., and
767 Denning, D.W. (2010). Azole antifungal resistance in *Aspergillus fumigatus*: 2008 and
768 2009. *J Antimicrob Chemother* *65*, 2116-2118. 10.1093/jac/dkq279.

769 7. Iversen, M., Burton, C.M., Vand, S., Skovfoged, L., Carlsen, J., Milman, N., Andersen,
770 C.B., Rasmussen, M., and Tvede, M. (2007). *Aspergillus* infection in lung transplant
771 patients: incidence and prognosis. *Eur J Clin Microbiol Infect Dis* *26*, 879-886.
772 10.1007/s10096-007-0376-3.

773 8. Lin, S.J., Schranz, J., and Teutsch, S.M. (2001). Aspergillosis case-fatality rate:
774 systematic review of the literature. *Clin Infect Dis* *32*, 358-366. 10.1086/318483.

- 775 9. Ward, R.A., and Vyas, J.M. (2020). The first line of defense: effector pathways of anti-
776 fungal innate immunity. *Curr Opin Microbiol* 58, 160-165. 10.1016/j.mib.2020.10.003.
- 777 10. Latgé, J.P., Beauvais, A., and Chamilos, G. (2017). The Cell Wall of the Human Fungal
778 Pathogen *Aspergillus fumigatus*: Biosynthesis, Organization, Immune Response, and
779 Virulence. *Annu Rev Microbiol* 71, 99-116. 10.1146/annurev-micro-030117-020406.
- 780 11. Valsecchi, I., Dupres, V., Michel, J.P., Duchateau, M., Matondo, M., Chamilos, G.,
781 Saveanu, C., Guijarro, J.I., Amanianda, V., Lafont, F., et al. (2019). The puzzling
782 construction of the conidial outer layer of *Aspergillus fumigatus*. *Cell Microbiol* 21,
783 e12994. 10.1111/cmi.12994.
- 784 12. Wang, Y., Aisen, P., and Casadevall, A. (1995). *Cryptococcus neoformans* melanin and
785 virulence: mechanism of action. *Infect Immun* 63, 3131-3136. 10.1128/iai.63.8.3131-
786 3136.1995.
- 787 13. Jahn, B., Koch, A., Schmidt, A., Wanner, G., Gehringer, H., Bhakdi, S., and Brakhage,
788 A.A. (1997). Isolation and characterization of a pigmentless-conidium mutant of
789 *Aspergillus fumigatus* with altered conidial surface and reduced virulence. *Infect Immun*
790 65, 5110-5117. 10.1128/iai.65.12.5110-5117.1997.
- 791 14. Langfelder, K., Jahn, B., Gehringer, H., Schmidt, A., Wanner, G., and Brakhage, A.A.
792 (1998). Identification of a polyketide synthase gene (pksP) of *Aspergillus fumigatus*
793 involved in conidial pigment biosynthesis and virulence. *Med Microbiol Immunol* 187, 79-
794 89.
- 795 15. Tsai, H.F., Chang, Y.C., Washburn, R.G., Wheeler, M.H., and Kwon-Chung, K.J. (1998).
796 The developmentally regulated *alb1* gene of *Aspergillus fumigatus*: its role in modulation
797 of conidial morphology and virulence. *J Bacteriol* 180, 3031-3038.
- 798 16. Sugareva, V., Hartl, A., Brock, M., Hubner, K., Rohde, M., Heinekamp, T., and
799 Brakhage, A.A. (2006). Characterisation of the laccase-encoding gene *abr2* of the
800 dihydroxynaphthalene-like melanin gene cluster of *Aspergillus fumigatus*. *Arch Microbiol*
801 186, 345-355. 10.1007/s00203-006-0144-2.
- 802 17. Chai, L.Y., Netea, M.G., Sugui, J., Vonk, A.G., van de Sande, W.W., Warris, A., Kwon-
803 Chung, K.J., and Kullberg, B.J. (2010). *Aspergillus fumigatus* conidial melanin modulates
804 host cytokine response. *Immunobiology* 215, 915-920. 10.1016/j.imbio.2009.10.002.
- 805 18. Akoumianaki, T., Kyrmizi, I., Valsecchi, I., Gresnigt, M.S., Samonis, G., Drakos, E.,
806 Boumpas, D., Muszkieta, L., Prevost, M.C., Kontoyiannis, D.P., et al. (2016). *Aspergillus*
807 cell wall melanin blocks LC3-associated phagocytosis to promote pathogenicity. *Cell*
808 *Host Microbe* 19, 79-90. 10.1016/j.chom.2015.12.002.
- 809 19. Goncalves, S.M., Duarte-Oliveira, C., Campos, C.F., Amanianda, V., Ter Horst, R.,
810 Leite, L., Mercier, T., Pereira, P., Fernandez-Garcia, M., Antunes, D., et al. (2020).
811 Phagosomal removal of fungal melanin reprograms macrophage metabolism to promote
812 antifungal immunity. *Nat Commun* 11, 2282. 10.1038/s41467-020-16120-z.
- 813 20. Kradin, R.L., and Mark, E.J. (2008). The pathology of pulmonary disorders due to
814 *Aspergillus spp.* *Arch Pathol Lab Med* 132, 606-614. 10.5858/2008-132-606-TPOPDD.

- 815 21. Latge, J.P. (2001). The pathobiology of *Aspergillus fumigatus*. Trends Microbiol 9, 382-
816 389. 10.1016/s0966-842x(01)02104-7.
- 817 22. Lee, J.Y., Joo, E.J., Yeom, J.S., Song, J.U., Yim, S.H., Shin, D.S., Yu, J.H., Ju, D.Y.,
818 Yim, J.W., Song, Y.S., et al. (2014). *Aspergillus* Tracheobronchitis and Influenza A Co-
819 infection in a Patient with AIDS and Neutropenia. Infect Chemother 46, 209-215.
820 10.3947/ic.2014.46.3.209.
- 821 23. Nyga, R., Maizel, J., Nseir, S., Chouaki, T., Milic, I., Roger, P.A., Van Grunderbeeck, N.,
822 Lemyze, M., Totet, A., Castelain, S., et al. (2020). Invasive Tracheobronchial
823 Aspergillosis in Critically Ill Patients with Severe Influenza. A Clinical Trial. Am J Respir
824 Crit Care Med 202, 708-716. 10.1164/rccm.201910-1931OC.
- 825 24. Montoro, D.T., Haber, A.L., Biton, M., Vinarsky, V., Lin, B., Birket, S.E., Yuan, F., Chen,
826 S., Leung, H.M., Villoria, J., et al. (2018). A revised airway epithelial hierarchy includes
827 CFTR-expressing ionocytes. Nature 560, 319-324. 10.1038/s41586-018-0393-7.
- 828 25. Yonker, L.M., Pazos, M.A., Lanter, B.B., Mou, H., Chu, K.K., Eaton, A.D., Bonventre,
829 J.V., Tearney, G.J., Rajagopal, J., and Hurley, B.P. (2017). Neutrophil-Derived Cytosolic
830 PLA2 α Contributes to Bacterial-Induced Neutrophil Transepithelial Migration. J Immunol
831 199, 2873-2884. 10.4049/jimmunol.1700539.
- 832 26. Feldman, M.B., Dutko, R.A., Wood, M.A., Ward, R.A., Leung, H.M., Snow, R.F., De La
833 Flor, D.J., Yonker, L.M., Reedy, J.L., Tearney, G.J., et al. (2020). *Aspergillus fumigatus*
834 Cell Wall Promotes Apical Airway Epithelial Recruitment of Human Neutrophils. Infect
835 Immun 88. 10.1128/IAI.00813-19.
- 836 27. Feldman, M.B., Wood, M., Lapey, A., and Mou, H. (2019). SMAD Signaling Restricts
837 Mucous Cell Differentiation in Human Airway Epithelium. Am J Respir Cell Mol Biol 61,
838 322-331. 10.1165/rcmb.2018-0326OC.
- 839 28. Yonker, L.M., Marand, A., Muldur, S., Hopke, A., Leung, H.M., De La Flor, D., Park, G.,
840 Pinsky, H., Guthrie, L.B., Tearney, G.J., et al. (2021). Neutrophil dysfunction in cystic
841 fibrosis. J Cyst Fibros 20, 1062-1071. 10.1016/j.jcf.2021.01.012.
- 842 29. Wang, Y., Aisen, P., and Casadevall, A. (1996). Melanin, melanin "ghosts," and melanin
843 composition in *Cryptococcus neoformans*. Infect Immun 64, 2420-2424.
844 10.1128/iai.64.7.2420-2424.1996.
- 845 30. Rosas, A.L., Nosanchuk, J.D., Feldmesser, M., Cox, G.M., McDade, H.C., and
846 Casadevall, A. (2000). Synthesis of polymerized melanin by *Cryptococcus neoformans*
847 in infected rodents. Infect Immun 68, 2845-2853. 10.1128/IAI.68.5.2845-2853.2000.
- 848 31. Folch, J., Lees, M., and Sloane Stanley, G.H. (1957). A simple method for the isolation
849 and purification of total lipides from animal tissues. J Biol Chem 226, 497-509.
- 850 32. Chamilos, G., Akoumianaki, T., Kyrmizi, I., Brakhage, A., Beauvais, A., and Latge, J.P.
851 (2016). Melanin targets LC3-associated phagocytosis (LAP): A novel pathogenetic
852 mechanism in fungal disease. Autophagy 12, 888-889.
853 10.1080/15548627.2016.1157242.

- 854 33. Camacho, E., Chrissian, C., Cordero, R.J.B., Liporagi-Lopes, L., Stark, R.E., and
855 Casadevall, A. (2017). N-acetylglucosamine affects *Cryptococcus neoformans* cell-wall
856 composition and melanin architecture. *Microbiology (Reading)* 163, 1540-1556.
857 10.1099/mic.0.000552.
- 858 34. Pazos, M.A., Lanter, B.B., Yonker, L.M., Eaton, A.D., Pirzai, W., Gronert, K., Bonventre,
859 J.V., and Hurley, B.P. (2017). *Pseudomonas aeruginosa* ExoU augments neutrophil
860 transepithelial migration. *PLoS Pathog* 13, e1006548. 10.1371/journal.ppat.1006548.
- 861 35. Yonker, L.M., Mou, H., Chu, K.K., Pazos, M.A., Leung, H., Cui, D., Ryu, J., Hibbler,
862 R.M., Eaton, A.D., Ford, T.N., et al. (2017). Development of a Primary Human Co-
863 Culture Model of Inflamed Airway Mucosa. *Sci Rep* 7, 8182. 10.1038/s41598-017-
864 08567-w.
- 865 36. Yonker, L.M., Pazos, M.A., Lanter, B.B., Mou, H., Chu, K.K., Eaton, A.D., Bonventre,
866 J.V., Tearney, G.J., Rajagopal, J., and Hurley, B.P. (2017). Neutrophil-Derived Cytosolic
867 PLA2alpha Contributes to Bacterial-Induced Neutrophil Transepithelial Migration. *J*
868 *Immunol* 199, 2873-2884. 10.4049/jimmunol.1700539.
- 869 37. Das, S.T., Rajagopalan, L., Guerrero-Plata, A., Sai, J., Richmond, A., Garofalo, R.P.,
870 and Rajarathnam, K. (2010). Monomeric and dimeric CXCL8 are both essential for *in*
871 *vivo* neutrophil recruitment. *PLoS One* 5, e11754. 10.1371/journal.pone.0011754.
- 872 38. Long, M.B., and Chalmers, J.D. (2022). Treating Neutrophilic Inflammation in Airways
873 Diseases. *Arch Bronconeumol* 58, 463-465. 10.1016/j.arbres.2021.11.003.
- 874 39. Tamang, D.L., Pirzai, W., Priebe, G.P., Traficante, D.C., Pier, G.B., Falck, J.R.,
875 Morisseau, C., Hammock, B.D., McCormick, B.A., Gronert, K., and Hurley, B.P. (2012).
876 Hepoxilin A(3) facilitates neutrophilic breach of lipoxygenase-expressing airway epithelial
877 barriers. *J Immunol* 189, 4960-4969. 10.4049/jimmunol.1201922.
- 878 40. Pazos, M.A., Pirzai, W., Yonker, L.M., Morisseau, C., Gronert, K., and Hurley, B.P.
879 (2015). Distinct cellular sources of hepoxilin A3 and leukotriene B4 are used to
880 coordinate bacterial-induced neutrophil transepithelial migration. *J Immunol* 194, 1304-
881 1315. 10.4049/jimmunol.1402489.
- 882 41. Mrsny, R.J., Gewirtz, A.T., Siccardi, D., Savidge, T., Hurley, B.P., Madara, J.L., and
883 McCormick, B.A. (2004). Identification of hepoxilin A3 in inflammatory events: a required
884 role in neutrophil migration across intestinal epithelia. *Proc Natl Acad Sci U S A* 101,
885 7421-7426. 10.1073/pnas.0400832101.
- 886 42. Kubala, S.A., Patil, S.U., Shreffler, W.G., and Hurley, B.P. (2014). Pathogen induced
887 chemo-attractant hepoxilin A3 drives neutrophils, but not eosinophils across epithelial
888 barriers. *Prostaglandins Other Lipid Mediat* 108, 1-8.
889 10.1016/j.prostaglandins.2013.11.001.
- 890 43. Riley, P.A. (1997). Melanin. *Int J Biochem Cell Biol* 29, 1235-1239. 10.1016/s1357-
891 2725(97)00013-7.
- 892 44. White, L.P. (1958). Melanin: a naturally occurring cation exchange material. *Nature* 182,
893 1427-1428. 10.1038/1821427a0.

- 894 45. Wheeler, M.H., and Bell, A.A. (1988). Melanins and their importance in pathogenic fungi.
895 Curr Top Med Mycol 2, 338-387. 10.1007/978-1-4612-3730-3_10.
- 896 46. Rhodes, J.C., Polacheck, I., and Kwon-Chung, K.J. (1982). Phenoloxidase activity and
897 virulence in isogenic strains of *Cryptococcus neoformans*. Infect Immun 36, 1175-1184.
898 10.1128/iai.36.3.1175-1184.1982.
- 899 47. Kwon-Chung, K.J., Tom, W.K., and Costa, J.L. (1983). Utilization of indole compounds
900 by *Cryptococcus neoformans* to produce a melanin-like pigment. J Clin Microbiol 18,
901 1419-1421. 10.1128/jcm.18.6.1419-1421.1983.
- 902 48. Salas, S.D., Bennett, J.E., Kwon-Chung, K.J., Perfect, J.R., and Williamson, P.R. (1996).
903 Effect of the laccase gene CNLAC1, on virulence of *Cryptococcus neoformans*. J Exp
904 Med 184, 377-386. 10.1084/jem.184.2.377.
- 905 49. Tsai, H.F., Washburn, R.G., Chang, Y.C., and Kwon-Chung, K.J. (1997). *Aspergillus*
906 *fumigatus* arp1 modulates conidial pigmentation and complement deposition. Mol
907 Microbiol 26, 175-183. 10.1046/j.1365-2958.1997.5681921.x.
- 908 50. Eisenman, H.C., Nosanchuk, J.D., Webber, J.B., Emerson, R.J., Camesano, T.A., and
909 Casadevall, A. (2005). Microstructure of cell wall-associated melanin in the human
910 pathogenic fungus *Cryptococcus neoformans*. Biochemistry 44, 3683-3693.
911 10.1021/bi047731m.
- 912 51. Eisenman, H.C., Mues, M., Weber, S.E., Frases, S., Chaskes, S., Gerfen, G., and
913 Casadevall, A. (2007). *Cryptococcus neoformans* laccase catalyses melanin synthesis
914 from both D- and L-DOPA. Microbiology (Reading) 153, 3954-3962.
915 10.1099/mic.0.2007/011049-0.
- 916 52. Stappers, M.H.T., Clark, A.E., Amanianda, V., Bidula, S., Reid, D.M., Asamaphan, P.,
917 Hardison, S.E., Dambuza, I.M., Valsecchi, I., Kerscher, B., et al. (2018). Recognition of
918 DHN-melanin by a C-type lectin receptor is required for immunity to *Aspergillus*. Nature
919 555, 382-386. 10.1038/nature25974.
- 920 53. Tam, J.M., Mansour, M.K., Khan, N.S., Yoder, N.C., and Vyas, J.M. (2012). Use of
921 fungal derived polysaccharide-conjugated particles to probe Dectin-1 responses in
922 innate immunity. Integr Biol (Camb) 4, 220-227. 10.1039/c2ib00089j.
- 923 54. Reedy, J.L., Crossen, A.J., Negoro, P.E., Harding, H.B., Ward, R.A., Vargas-Blanco,
924 D.A., Timmer, K.D., Reardon, C.M., Basham, K.J., Mansour, M.K., et al. (2023). The C-
925 Type Lectin Receptor Dectin-2 Is a Receptor for *Aspergillus fumigatus* Galactomannan.
926 mBio 14, e0318422. 10.1128/mbio.03184-22.
- 927 55. Chow, A.W., Liang, J.F., Wong, J.S., Fu, Y., Tang, N.L., and Ko, W.H. (2010). Polarized
928 secretion of interleukin (IL)-6 and IL-8 by human airway epithelia 16HBE14o- cells in
929 response to cationic polypeptide challenge. PLoS One 5, e12091.
930 10.1371/journal.pone.0012091.
- 931 56. Pillai, D.K., Sankoorikal, B.J., Johnson, E., Seneviratne, A.N., Zurko, J., Brown, K.J.,
932 Hathout, Y., and Rose, M.C. (2014). Directional secretomes reflect polarity-specific

- 933 functions in an in vitro model of human bronchial epithelium. *Am J Respir Cell Mol Biol*
934 50, 292-300. 10.1165/rcmb.2013-0188OC.
- 935 57. Skronska-Wasek, W., Durlanik, S., Garnett, J.P., and Pflanz, S. (2021). Polarized
936 cytokine release from airway epithelium differentially influences macrophage phenotype.
937 *Mol Immunol* 132, 142-149. 10.1016/j.molimm.2021.01.029.
- 938 58. Hurley, B.P., Siccardi, D., Mrsny, R.J., and McCormick, B.A. (2004). Polymorphonuclear
939 cell transmigration induced by *Pseudomonas aeruginosa* requires the eicosanoid
940 heptaxilin A3. *J Immunol* 173, 5712-5720. 10.4049/jimmunol.173.9.5712.
- 941 59. Kusek, M.E., Pazos, M.A., Pirzai, W., and Hurley, B.P. (2014). *In vitro* coculture assay to
942 assess pathogen induced neutrophil trans-epithelial migration. *J Vis Exp*, e50823.
943 10.3791/50823.
- 944 60. Crossen, A.J., Ward, R.A., Reedy, J.L., Surve, M.V., Klein, B.S., Rajagopal, J., and
945 Vyas, J.M. (2022). Human Airway Epithelium Responses to Invasive Fungal Infections:
946 A Critical Partner in Innate Immunity. *J Fungi (Basel)* 9. 10.3390/jof9010040.
- 947 61. Chamilos, G., and Carvalho, A. (2020). *Aspergillus fumigatus* DHN-Melanin. *Curr Top*
948 *Microbiol Immunol* 425, 17-28. 10.1007/82_2020_205.
- 949 62. Kyrmizi, I., Ferreira, H., Carvalho, A., Figueroa, J.A.L., Zampas, P., Cunha, C.,
950 Akoumianaki, T., Stylianou, K., Deepe, G.S., Jr., Samonis, G., et al. (2018). Calcium
951 sequestration by fungal melanin inhibits calcium-calmodulin signalling to prevent LC3-
952 associated phagocytosis. *Nat Microbiol* 3, 791-803. 10.1038/s41564-018-0167-x.
- 953 63. Nosanchuk, J.D., and Casadevall, A. (2003). The contribution of melanin to microbial
954 pathogenesis. *Cell Microbiol* 5, 203-223. 10.1046/j.1462-5814.2003.00268.x.
- 955 64. Levardon, H., Yonker, L.M., Hurley, B.P., and Mou, H. (2018). Expansion of Airway
956 Basal Cells and Generation of Polarized Epithelium. *Bio Protoc* 8.
957 10.21769/BioProtoc.2877.
- 958 65. Mou, H., Vinarsky, V., Tata, P.R., Brazauskas, K., Choi, S.H., Crooke, A.K., Zhang, B.,
959 Solomon, G.M., Turner, B., Bihler, H., et al. (2016). Dual SMAD Signaling Inhibition
960 Enables Long-Term Expansion of Diverse Epithelial Basal Cells. *Cell Stem Cell* 19, 217-
961 231. 10.1016/j.stem.2016.05.012.
- 962 66. Mou, H., Yang, Y., Riehs, M.A., Barrios, J., Shivaraju, M., Haber, A.L., Montoro, D.T.,
963 Gilmore, K., Haas, E.A., Paunovic, B., et al. (2021). Airway basal stem cells generate
964 distinct subpopulations of PNECs. *Cell Rep* 35, 109011. 10.1016/j.celrep.2021.109011.
- 965 67. Rossner, M., and Yamada, K.M. (2004). What's in a picture? The temptation of image
966 manipulation. *J Cell Biol* 166, 11-15. 10.1083/jcb.200406019.
- 967

Figure 1

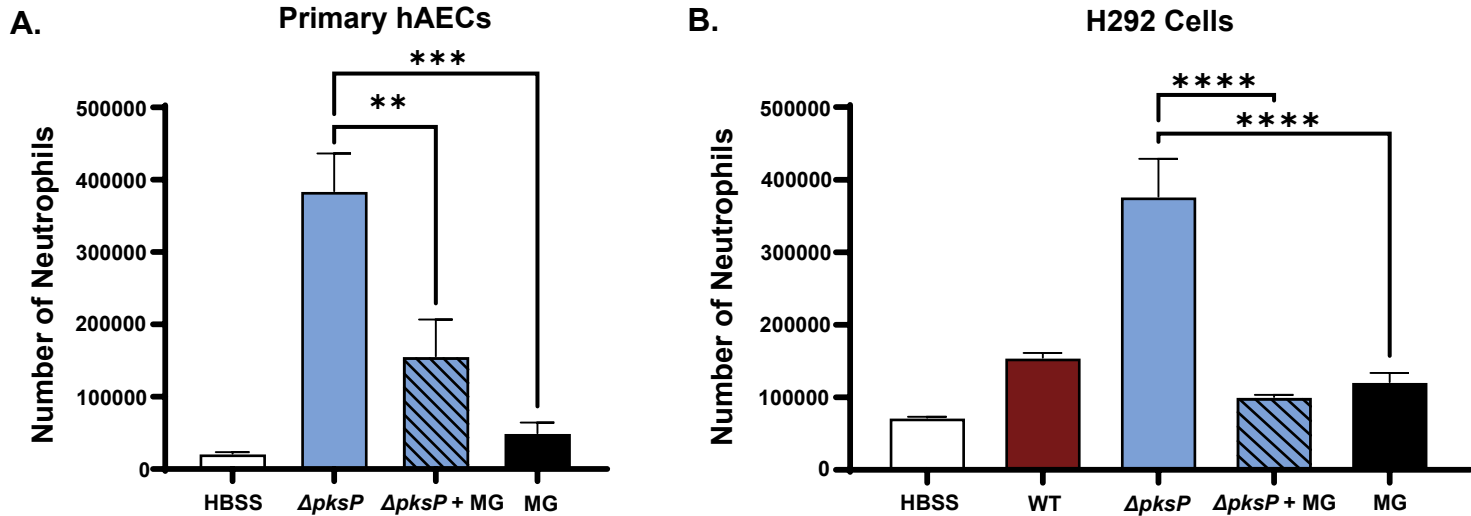


Figure 2

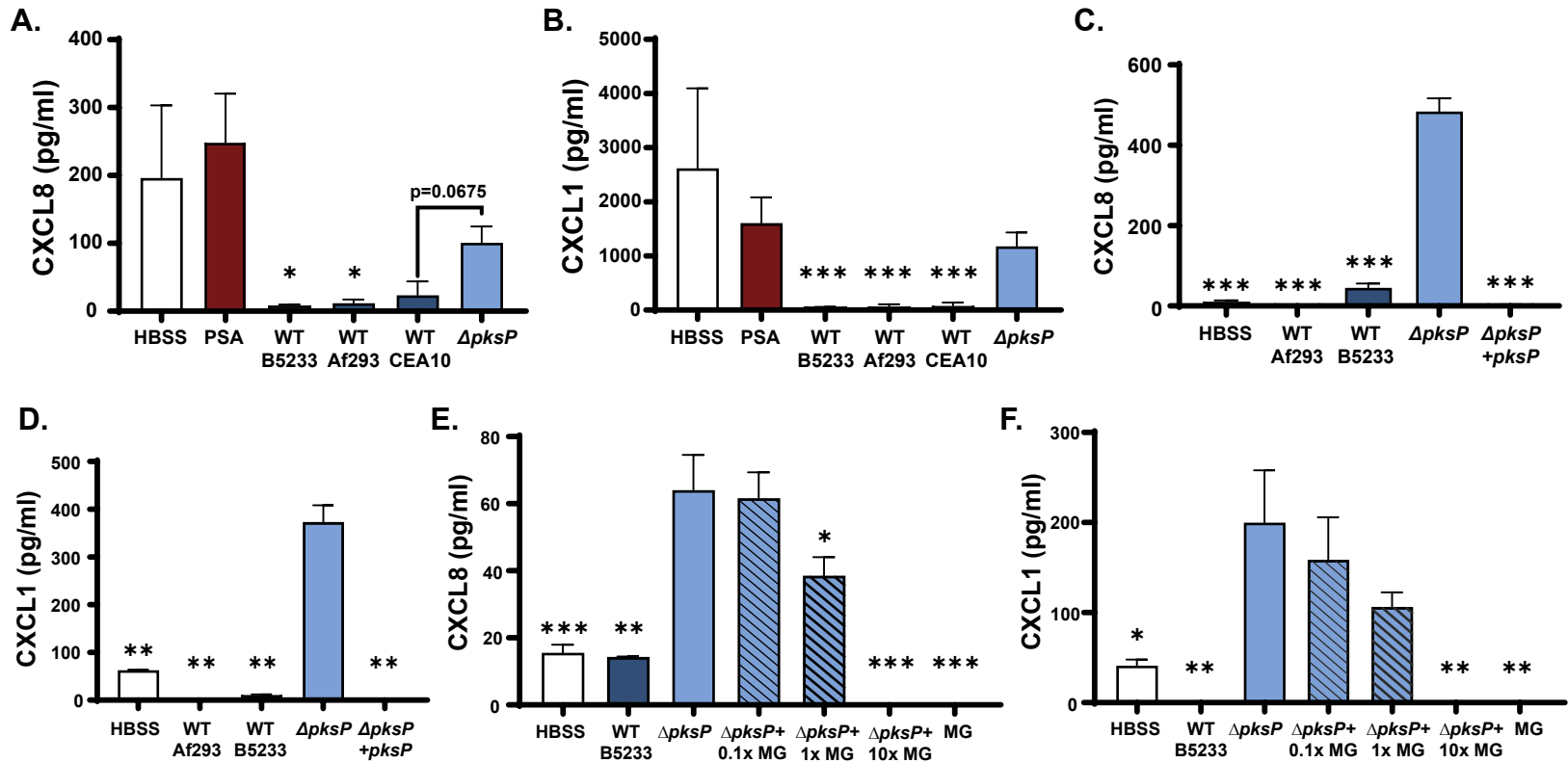


Figure 3

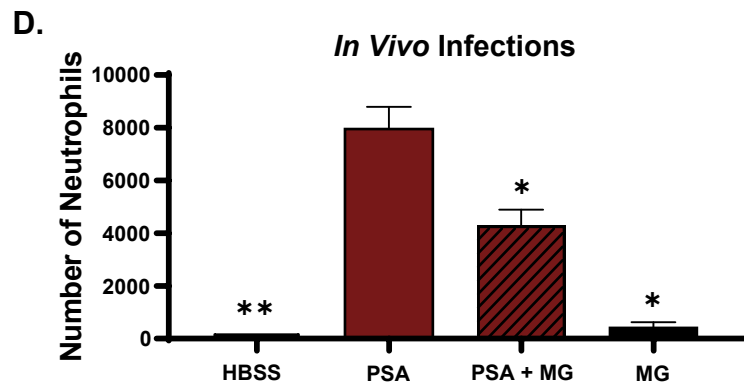
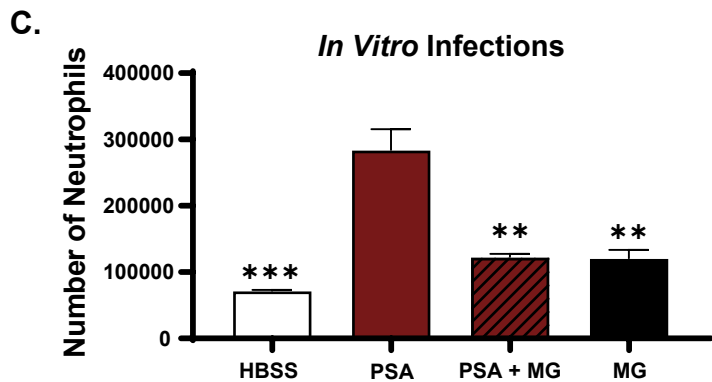
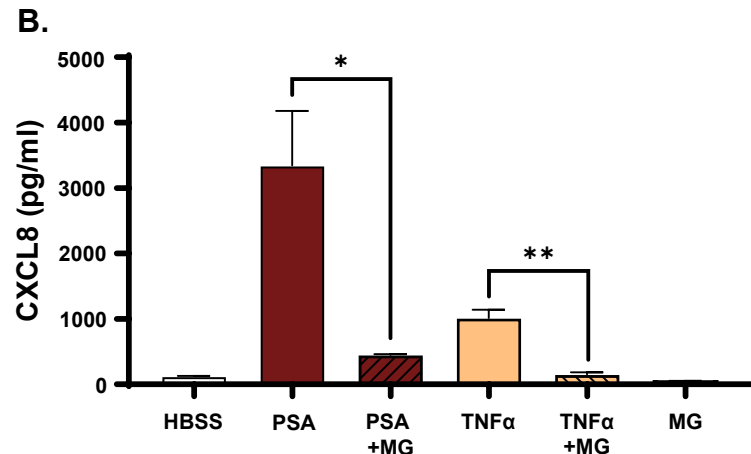
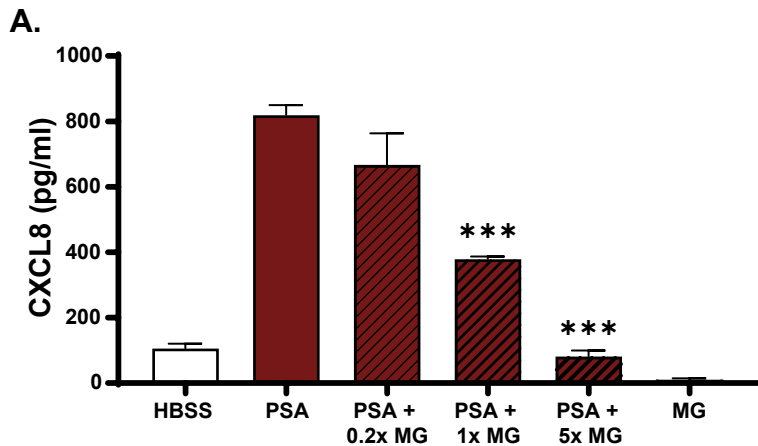
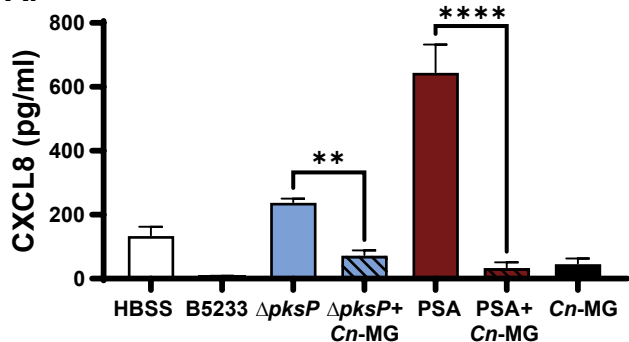


Figure 4

A.



B.

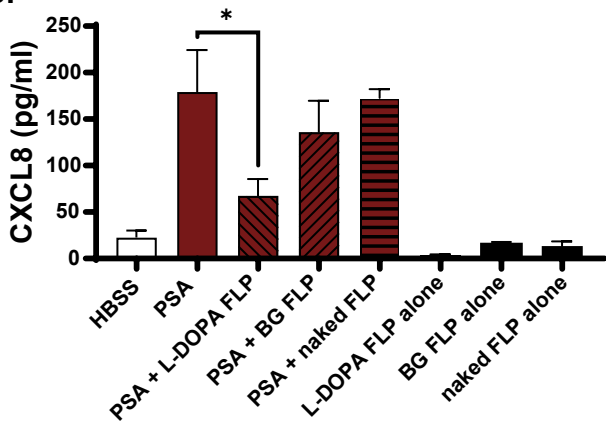
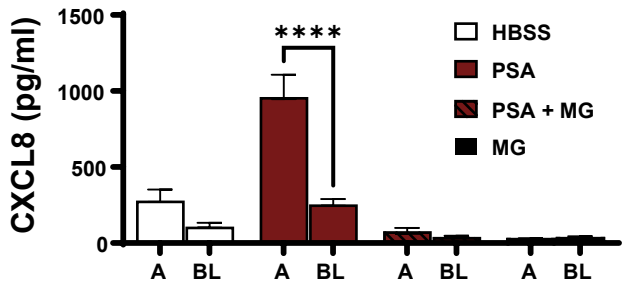


Figure 5

A.



B.

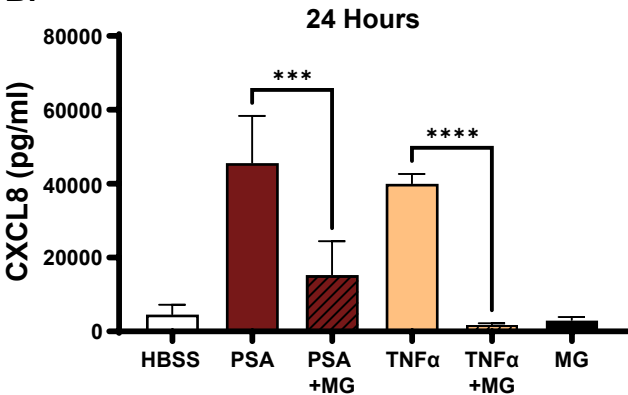


Figure 6

